Journal of Biomechanics 82 (2019) 392–396

Contents lists available at ScienceDirect

Journal of Biomechanics

journal homepage: www.elsevier.com/locate/jbiomech
www.JBiomech.com

Simulating contact using the elastic foundation algorithm in OpenSim ☆

Michael W. Hast [a,*], Brett G. Hanson [a], Josh R. Baxter [b]

[a] Biedermann Lab for Orthopaedic Research, Department of Orthopaedic Surgery, The University of Pennsylvania, Philadelphia, PA 19104, USA
[b] Human Motion Lab, Department of Orthopaedic Surgery, The University of Pennsylvania, Philadelphia, PA 19104, USA

ARTICLE INFO

Article history:
Accepted 8 November 2018

Keywords:
Computational simulation
Contact forces
Tibiofemoral forces

ABSTRACT

Modeling joint contact in OpenSim is not well understood. This study systematically investigated the variables associated with the elastic foundation contact model within OpenSim by performing a series of controlled benchtop experiment and concomitant simulations. Four metal-on-plastic interactions were modeled, including a model of a total knee replacement (TKR). Load-displacement curves were recorded during cyclic loading between 100 and 750 N. Geometries were imported and into OpenSim and contact mechanics were modeled with the on-board elastic foundation algorithm. A hybrid optimization algorithm determined that stiffness and dissipation coefficients for TKR implants were 1.52×10^{10} N/m and 57.7 Ns/m, respectively. Estimations of contact forces were 10.2% of blinded experimental data (average root mean square error: 76.82 ± 11.47 N). In the second portion of this study, freely available eTibia TKR renderings were used to test the ubiquity of the tuning parameters. They were also used to perform a sensitivity analysis of material stiffness and mesh density with regard to penetration depth and computational time. When a stiffness of 1×10^{10} was applied to an eTibia model with 5000 faces, a 100 kg load caused 0.259 mm of penetration. Under the same conditions, the tuned model experienced 0.300 mm of penetration. Material stiffnesses between 1×10^{13} and 1×10^{15} N/m increased computation time by factors of 12–23. This study provides much needed clarity regarding the use of the OpenSim EF algorithm. It also demonstrates the utility of OpenSim to model deformable materials and complex geometries, and this approach can be adapted to make reasonable estimations for both natural and surgically modified joints.

1. Introduction

Predicting articular joint function and loading continues to be an important research topic in orthopaedics. Effective clinical treatment and design of orthopaedic implants requires a thorough understanding of joint loads throughout dynamic activities of daily living. Computer simulation has become a widely used method for the determination of joint contact forces during dynamic tasks, as it is not subject to the same constraints that accompany physical experimental investigations. Traditionally, joint contact modeling has been performed using deformable finite element models, but these simulations are mathematically complex and computationally expensive (Giddings et al., 2001; Godest et al., 2002; Halloran et al., 2005). In the mid-2000′s an alternative option for modeling contact, known as the elastic foundation (EF) paradigm, became a commonly utilized approach. Although EF may over approximate contact pressures when compared to similar finite element models, EF calculations are comparatively inexpensive with respect to computational cost, a desirable characteristic for integrating joint contact into muscle-driven simulations (Kim et al., 2009; Lenhart et al., 2015; Lin and Fregly, 2010; Schmitz and Piovesan, 2016; Shelburne et al., 2006; Taylor et al., 2004). Recently, even faster options have been developed by leveraging surrogate contact modeling paradigms (Eskinazi and Fregly, 2015; Lin and Fregly, 2010).

OpenSim (Delp et al., 2007) is a widely used and freely available musculoskeletal modeling software package. Released in 2007, OpenSim can be used to solve both kinematic and inverse dynamic simulations of human motion. This software package has an onboard EF contact algorithm that provides users the functionality to estimate contact between two geometries, which can be represented as either simple shapes or complex mesh-based geometries. Based on the history of forum posts, this OpenSim feature is not well understood by many users (Dunne et al., 2017a, b, 2013).

☆ Study conducted at The University of Pennsylvania, Philadelphia, Pennsylvania, USA.

* Corresponding author at: Biedermann Lab for Orthopaedic Research, 3737 Market Street, 10th Floor Suite 1050, The University of Pennsylvania, Philadelphia, PA 19104, USA.

E-mail address: hast@pennmedicine.upenn.edu (M.W. Hast).

https://doi.org/10.1016/j.jbiomech.2018.11.025
0021-9290/

Although the mathematical concept behind the EF algorithm is outlined in several publications (Flores and Lankarani, 2016; Machado et al., 2010; Sherman et al., 2011; Uchida et al., 2015), details regarding validation and implementation remain confusing for end users. For example, the material stiffness and dissipation coefficients are complex in nature (derived in Appendix A of (Sherman et al., 2011)), and are described as follows:

Stiffness:

"At the centroid of each triangle on each surface is placed a spring whose stiffness k can be determined from the area of its triangle, the composite material property E^* and thickness h."

Dissipation:

"A Hunt and Crossley-like dissipation term $kx(c^*\dot{x})$ is added to complete the normal force..."

Aside from confusion regarding input parameters, measures of accuracy and computation time have yet to be investigated for the OpenSim EF algorithm. Although it is well known that mesh density and geometric complexity greatly affect computational time and accuracy (Bei and Fregly, 2004), no study has quantified these variables within the OpenSim framework.

The purpose of the present work was to systematically investigate the variables associated with the EF algorithm in OpenSim, such that estimations of joint contact forces can be made quickly, accurately and with confidence. To do this, a simple set of physical experiments and concomitant OpenSim models were developed to examine sensitivities regarding model geometry, EF input parameters, and model outputs. Second, we utilized an open-source model of total knee replacement (TKR) components to test the ubiquity of the determined coefficients and to assess the relationships between mesh density, penetration, stiffness, and simulation time.

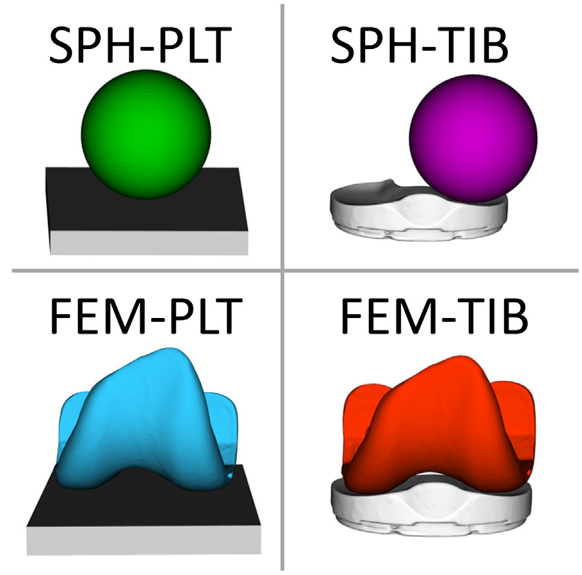

Fig. 1. 3-D renderings of the four different combinations of a sphere, plate, TKR femur, and TKR tibia used in the experiment. Acronyms used in other figures are listed above each pairing.

Table 1
Summary of 3-D rending models.

Component	Number of faces	Number of vertices
Sphere	5852	2928
Plate	30,208	15,106
Femur	20,000	10,002
Tibia	20,000	10,002

2. Methods

2.1. Tuning and testing contact parameters

Four separate physical experiments were performed using a 316L stainless steel sphere (5.08 cm diameter), a plate of commercial ultra high molecular weight polyethylene (UHMWPE – 15.24 L × 7.62 W × 0.95H cm), a TKR femoral component, and a TKR tibial insert (Size 4, Triathlon, Stryker, Mahwah, NJ). The plastic and metal components were combined together to make the following pairings: sphere-on-plate, sphere-on-tibia, femur-on-plate, femur-on-tibia (Fig. 1). The plastic components were placed on the bed of the test frame (Electroforce 3330, TA Instruments, New Castle, DE) and the metal components were compressed upon the bearing surfaces under load control. To simulate dynamic loading, the actuator imparted loads between 100 and 750 N at 1 Hz for 1000 cycles. Force-displacement data were collected at 100 Hz. Trials were repeated 4 times for each group.

Three-dimensional (3-D) renderings of the various parts were created by either drafting them in Solidworks (2017, Dassault Systèmes, Waltham, MA), or scanning them with a 3-D optical scanner (Einscan SE, Shining 3D, Hangzhou, China). Mesh geometries were either coarsened or subdivided with Meshlab (Cignoni et al., 2008)) and the resulting renderings ranged in size between 5852 and 30,208 faces (Table 1). Geometries were imported into OpenSim (version 3.3) and defined in an EF contact model (Appendix A).

Stiffness and dissipation constants were tuned by using a novel optimization algorithm. 10 cycles of experimental load displacement data were used as input. To minimize the effects of preconditioning and hysteresis, cycles 1–979 of the test were omitted from the analysis. The force-displacement profiles of the 980th–989th trials were used to tune the computational model. Actuator displacements measured during the physical experiment were used as inputs of prescribed motion of the metallic component. Contact forces between the two bodies were calculated in OpenSim with the onboard Force Reporter algorithm (Sherman et al., 2011). Force versus time curves were constructed for the physical experiment and simulation. Root mean square errors (RMSE) between these two curves were used as an objective function. For each experimental trial, the values of stiffness and dissipation were optimized using a hybrid "particleswarm/fmincon" function (MATLAB, The Mathworks, Natick, MA) until the RMSE was minimized, which took between 30 and 120 min of computational time. The upper and lower bounds for the stiffness and dissipation coefficients were set to [1e8–1e12] and [0–100], respectively. For each test condition, final stiffnesses and dissipations were averaged to create optimized parameter values. Finally, using the averaged parameters, the experimental displacements of the 990th–999th cycles were prescribed in a new simulation and the resulting contact forces were estimated. The 1000th cycle was omitted because completion of the last cycle in physical experiment was not consistent across trials. To assess tuning accuracy, the newly estimated force versus time curves were compared to their experimentally measured counterparts by calculating the RMSE of the two curves.

2.2. Evaluating contact simulation performance

Using freely available 3-D renderings of TKR components (eTibia (Fregly et al., 2012)), tibiofemoral contact was modeled using a forward dynamic simulation for two purposes. First, to assess the ubiquity of the results from the previous experiment when applied to a different TKR geometry. Second, to quantify the relationships between computation time, implant penetration, material stiffness, and mesh density. To achieve these goals, component geometries were imported into OpenSim and contact was modeled as an elastic foundation element. 'Drop and settle' simulations, where the femoral component was dropped upon the tibial component from a 1 mm height. Based on results from the first half of this study, simulations were performed over a series of model configurations to test the effects of tibial insert stiffness (1×10^9 to 1×10^{15} N/m) mesh coarseness (100, 500, 1000, 2500, and 5000 faces), and computational time in an effort to minimize computational time. Different amounts of weight bearing were also simulated by changing the mass of the femoral component (1, 10, and 100 kg). Center of mass position was adjusted to eliminate rotation of the femoral component during simulations. Component penetration was calculated as the vertical change in position of the femoral component center of mass from the point of initial component contact to the final settling position. In total, 105 simulations were performed on a personal computer (Intel Core i5-6500, 3.20 GHz, 8 GB RAM).

3. Results and discussion

The tuning optimization yielded average stiffness values that were substantially different for each metal-on-plastic pairing (Fig. 2A, Appendix B). The average stiffness value for the sphere-on-plate group (3.01×10^{11} N/m) and sphere-on-tibia group (1.12×10^{11} N/m) were an order of magnitude higher than the stiffness values for the femur-on-plate (3.79×10^{10} N/m) and femur-on-tibia (1.52×10^{10} N/m). These changes are likely due to differences in contact patch areas, as the sphere-on-plate simulations had a single patch of minimal size, while femur-on-tibia simulations had a high degree of bicondylar conformity. Estimations of stiffness for experiments using the tibial component had some variability, whereas simulations involving a plate had almost none. Dissipation values were less consistent than stiffness estimations, but changes to these values resulted in minimal changes to the RMSE (Fig. 2B). Results from this portion of the study demonstrate that contact mechanics of metal-on-plastic bearings are largely dependent upon the stiffness coefficient, whereas the dissipation coefficient plays a minimal role (Fig. 3A, Appendix C).

The optimization routine presented in this paper accurately predicted forces associated with blinded experimental displacements (Table 2). When pooling the results of all 16 experimental and simulated force versus time curves, the average root mean squared error (RMSE) was 53.11 ± 34.46 N, or 7.1 ± 4.6% error of the maximum applied load of 750 N. RMSE values were smaller when the plates were used as a bearing surface (sphere-on-plate 20.84 ± 2.18 N; femur-on-plate 45.33 ± 2.64 N) compared to when the tibial component was used (sphere-on-tibia 69.46 ± 60.11 N; femur-on-tibia 76.83 ± 11.47 N). This result is likely caused by small changes in the experimental force-displacement profile that changed due to small perturbations in tibial component alignment before testing. This phenomena does not exist in tests with flat plates.

Simulated eTibia tibiofemoral penetrations compared favorably to the tuned TKR model. For example, when a stiffness of 1×10^{10} was applied to eTibia models with 1000, 2500, and 5000 faces, a 100 kg load caused 0.223, 0.245, and 0.259 mm of penetration, respectively (Fig. 3B). The tuned femur-on-tibia model experienced 0.300 mm of penetration when subjected to the same load. In general, the eTibia simulations provided reasonable amounts of penetration when the stiffness was set between 1×10^{10} and 1×10^{12} N/m and the contact mesh had at least 1000 faces. Lower stiffness values (1×10^9 N/m) and higher stiffness values (1×10^{13} to 1×10^{15} N/m) resulted in non-physiologic penetrations of greater than 0.5 mm and component chattering, respectively.

Computation time increased as a function of both material stiffness and mesh density; however, overly stiff (1×10^{14}–1×10^{15} N/m) increased by a factor of 12–23 times longer than simulations with 1×10^{11} N/m (Fig. 3C). Overly high stiffness coefficients drastically increased computation time and created chattering behaviors between the contacting bodies, which was an artifact of increased joint reaction loads (Appendix C). Mesh size also played an important role in overall simulation performance. Course meshes resulted in increased component penetration and fine meshes increased computation time unnecessarily.

This experiment has several limitations. The cyclic axial load of 750 N at 1 Hz was chosen because it represents approximately one body weight of a 50th percentile male, but it does not account for rotations and sliding of the joint, nor does it account for different loading velocities. The small contact patch between the plate and sphere resulted in slightly higher maximum contact pressures (24.97 ± 4.04 MPa, Appendix D) than reported in TKA (~19 MPa) (Kwon et al., 2014). At the same time, the application of 750 N to the femur-on-tibia pairing underestimates the 2.5–2.8 body weights of load applied to the knee during walking (D'Lima et al., 2012). The parameters of static, dynamic, and viscous friction were all assumed to be negligent and therefore were set to zero (Hast and Piazza, 2013; Thompson et al., 2011). This may not be the case

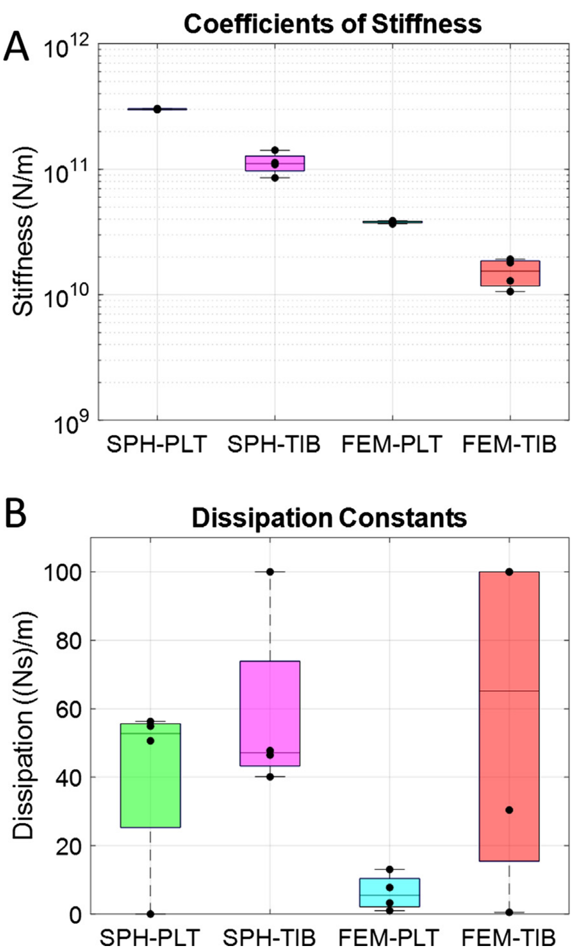

Fig. 2. Boxplots showing the (A) stiffness and (B) dissipation coefficients that were determined for the four groups tested. Substantial changes in stiffness coefficients were measured across the four groups, and variability was small when the plate was used as the bearing surface. Dissipation coefficients did not follow similar trends.

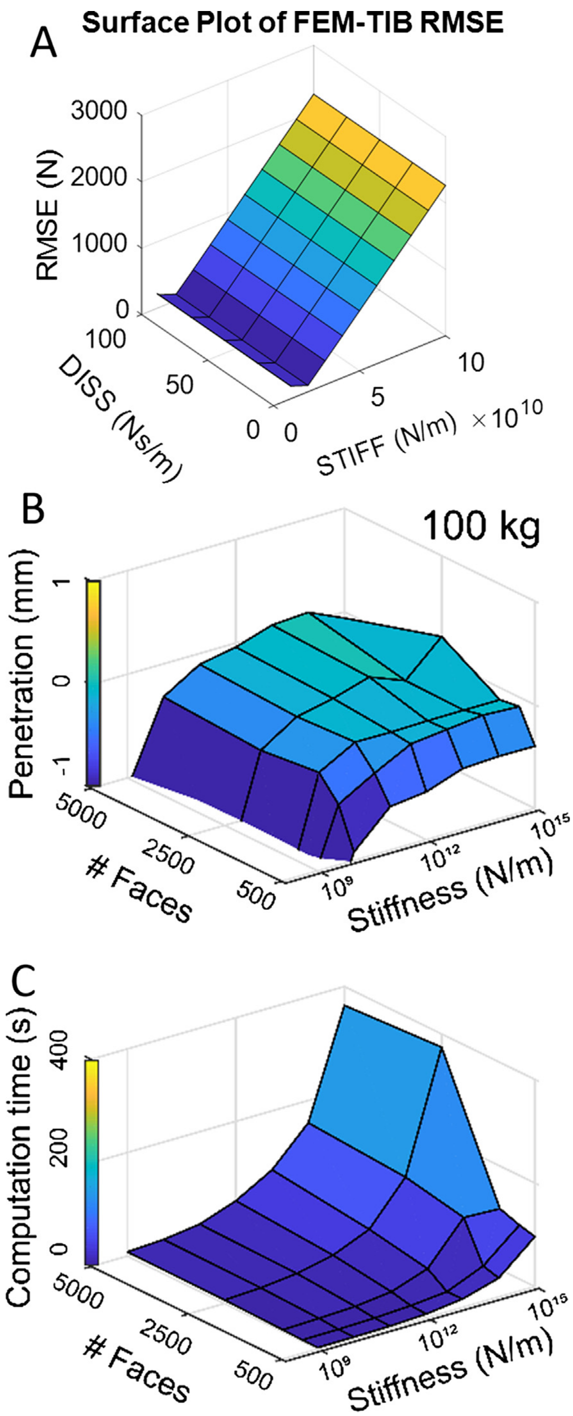

Fig. 3. Surface plots showing the (A) changes in RMSE (B) component penetration, and (C) computation time, relative to changes in the number of faces in the model, stiffness, and dissipation coefficients. RMSE was more sensitive to stiffness than dissipation. Penetrations were more sensitive to material stiffness than the mesh density (# faces). Low stiffness constants resulted in excess penetration (negative values) and increased computation time.

for more complex motions, and the parameters could readily be added to the optimization routine.

4. Conclusions

OpenSim provides an EF algorithm that is freely available, computationally light, and potentially powerful, but the tool is vastly underutilized because it is poorly understood. This experiment represents the first published work that has outlined a rigorous experimental approach to determine parameters for the OpenSim EF algorithm when assessing both simple geometries and TKR components. If future researchers are unable to recapitulate this experimental approach for exact implant geometries, stiffness and dissipation coefficients of 1.52×10^{10} N/m and 57.7 Ns/m provide reasonable TKR contact mechanics in the OpenSim EF algorithm. Generally speaking, model complexity and contact patch area play important roles in the determination of accurate EF input parameters. If mesh density and stiffness parameters are tuned appropriately, simulations will run quickly without sacrificing accuracy. Because the EF algorithm within OpenSim is easily adapted to model soft tissues and complex geometries, the same overall approach can be straightforwardly adapted to make reasonable estimations of contact forces for both natural and surgically modified joints throughout the body.

Table 2
Summary of RMSE values for each simulation.

Trial	RMSE (N)	Trial	RMSE (N)
Sphere on Plate 1	21.26	Sphere on Tibia 1	142.60
Sphere on Plate 2	20.74	Sphere on Tibia 2	19.86
Sphere on Plate 3	23.33	Sphere on Tibia 3	20.58
Sphere on Plate 4	18.04	Sphere on Tibia 4	94.78
Average	20.84	Average	69.46
Standard deviation	2.18	Standard deviation	60.11
Femur on Plate 1	48.51	Femur on Tibia 1	90.11
Femur on Plate 2	42.21	Femur on Tibia 2	78.37
Femur on Plate 3	44.58	Femur on Tibia 3	76.72
Femur on Plate 4	46.03	Femur on Tibia 4	62.12
Average	45.33	Average	76.83
Standard deviation	2.64	Standard deviation	11.47

Acknowledgement

The authors would like to thank the Biedermann family, who provided funding for this study.

Conflict of interest statement

Michael Hast has sponsored research agreements with DePuy Synthes, Zimmer Biomet, and Integra LifeSciences. None of these are relevant to the submission.

Brett Hanson has no conflicts to disclose.

Josh Baxter has no conflicts to disclose.

Appendix A. Supplementary material

Supplementary data to this article can be found online at https://doi.org/10.1016/j.jbiomech.2018.11.025.

References

Bei, Y., Fregly, B.J., 2004. Multibody dynamic simulation of knee contact mechanics. Med. Eng. Phys. 26, 777–789.
Cignoni, P., Callieri, M., Corsini, M., Dellepiane, M., Ganovelli, F., Ranzuglia, G., 2008. MeshLab: an open-source mesh processing tool. In: Scarano, V., Chiara, R.D., Erra, U. (Eds.), Eurographics Italian Chapter Conference. The Eurographics Association.
Delp, S.L., Anderson, F.C., Arnold, A.S., Loan, P., Habib, A., John, C.T., Guendelman, E., Thelen, D.G., 2007. OpenSim: open-source software to create and analyze dynamic simulations of movement. Biomed. Eng., IEEE Trans. 54, 1940–1950.
D'Lima, D.D., Fregly, B.J., Patil, S., Steklov, N., Colwell, C.W., 2012. Knee joint forces: prediction, measurement, and significance. Proc. Inst. Mech. Eng. H 226, 95–102.
Dunne, J., Ku, J., Seth, A., Delp, S.L., Hicks, J.L., Habib, A., Uchida, T., Pineda, B., 2017a. OpenSim Forum: Elastic Foundation Model [WWW Document]. URL https://

simtk.org/plugins/phpBB/viewtopicPhpbb.php?f=91&t=8380&p=22928&start=0&view=&sid=50dd5809b3bdb48c8c9525315c31eb30

Dunne, J., Ku, J., Seth, A., Delp, S.L., Hicks, J.L., Habib, A., Uchida, T., Pineda, B., 2017b. OpenSim Forum: Penetrating Surfaces Between Triangular Meshes [WWW Document]. URL https://simtk.org/plugins/phpBB/viewtopicPhpbb.php?f=91&t=8380&p=22928&start=0&view=&sid=50dd5809b3bdb48c8c9525315c31eb30

Dunne, J., Ku, J., Seth, A., Delp, S.L., Hicks, J.L., Habib, A., Uchida, T., Pineda, B., 2013. OpenSim Forum: Trouble with Contact [WWW Document]. URL https://simtk.org/plugins/phpBB/viewtopicPhpbb.php?f=91&t=4404&p=16330&start=0&view=&sid=d8ccc62b05f6a94be41cf458211008fc

Eskinazi, I., Fregly, B.J., 2015. Surrogate modeling of deformable joint contact using artificial neural networks. Med. Eng. Phys. 37, 885–891.

Flores, P., Lankarani, H.M., 2016. Contact Force Models for Multibody Dynamics, Solid Mechanics and Its Applications. Springer International Publishing.

Fregly, B.J., Besier, T.F., Lloyd, D.G., Delp, S.L., Banks, S.A., Pandy, M.G., D'Lima, D.D., 2012. Grand challenge competition to predict in vivo knee loads. J. Orthop. Res. 30, 503–513.

Giddings, V.L., Kurtz, S.M., Edidin, A.A., 2001. Total knee replacement polyethylene stresses during loading in a knee simulator. J. Tribol. 123, 842–847.

Godest, A.C., Beaugonin, M., Haug, E., Taylor, M., Gregson, P.J., 2002. Simulation of a knee joint replacement during a gait cycle using explicit finite element analysis. J. Biomech. 35, 267–275.

Halloran, J.P., Easley, S.K., Petrella, A.J., Rullkoetter, P.J., 2005. Comparison of deformable and elastic foundation finite element simulations for predicting knee replacement mechanics. J. Biomech. Eng. 127, 813–818.

Hast, M.W., Piazza, S.J., 2013. Dual-joint modeling for estimation of total knee replacement contact forces during locomotion. J. Biomech. Eng. 135, 021013.

Kim, H.J., Fernandez, J.W., Akbarshahi, M., Walter, J.P., Fregly, B.J., Pandy, M.G., 2009. Evaluation of predicted knee-joint muscle forces during gait using an instrumented knee implant. J. Orthop. Res. 27, 1326–1331.

Kwon, O.-R., Kang, K.-T., Son, J., Kwon, S.-K., Jo, S.-B., Suh, D.-S., Choi, Y.-J., Kim, H.-J., Koh, Y.-G., 2014. Biomechanical comparison of fixed- and mobile-bearing for unicomparmental knee arthroplasty using finite element analysis. J. Orthop. Res. 32, 338–345.

Lenhart, R.L., Smith, C.R., Vignos, M.F., Kaiser, J., Heiderscheit, B.C., Thelen, D.G., 2015. Influence of step rate and quadriceps load distribution on patellofemoral cartilage contact pressures during running. J. Biomech. 48, 2871–2878.

Lin, Y.C., Fregly, B.J., 2010. Surrogate articular contact models for computationally efficient multibody dynamic simulations. Med. Eng. Phys. 32, 584.

Machado, M., Flores, P., Claro, J.C.P., Ambrósio, J., Silva, M., Completo, A., Lankarani, H.M., 2010. Development of a planar multibody model of the human knee joint. Nonlinear Dyn. 60, 459–478.

Schmitz, A., Piovesan, D., 2016. Development of an open-source, discrete element knee model. IEEE Trans. Biomed. Eng. 63, 2056–2067.

Shelburne, K.B., Torry, M.R., Pandy, M.G., 2006. Contributions of muscles, ligaments, and the ground-reaction force to tibiofemoral joint loading during normal gait. J. Orthop. Res. 24, 1983–1990.

Sherman, M.A., Seth, A., Delp, S.L., 2011. Simbody: multibody dynamics for biomedical research. Procedia IUTAM 2, 241–261.

Taylor, W.R., Heller, M.O., Bergmann, G., Duda, G.N., 2004. Tibio-femoral loading during human gait and stair climbing. J. Orthop. Res. 22, 625–632.

Thompson, J.A., Hast, M.W., Granger, J.F., Piazza, S.J., Siston, R.A., 2011. Biomechanical effects of total knee arthroplasty component malrotation: a computational simulation. J. Orthop. Res.

Uchida, T.K., Sherman, M.A., Delp, S.L., 2015. Making a meaningful impact: modelling simultaneous frictional collisions in spatial multibody systems. Proc. Math. Phys. Eng. Sci. 471, 20140859.